

SCIENTIFIC REPORTS



OPEN

Impairment of starch biosynthesis results in elevated oxidative stress and autophagy activity in *Chlamydomonas reinhardtii*

Quynh-Giao Tran^{1,2}, Kichul Cho³, Su-Bin Park^{1,2}, Urim Kim^{1,2}, Yong Jae Lee¹ & Hee-Sik Kim^{1,2}

Autophagy is a self-degradation system wherein cellular materials are recycled. Although autophagy has been extensively studied in yeast and mammalian systems, integrated stress responses in microalgae remain poorly understood. Accordingly, we carried out a comparative study on the oxidative stress responses of *Chlamydomonas reinhardtii* wild-type and a starchless (*sta6*) mutant previously shown to accumulate high lipid content under adverse conditions. To our surprise, the *sta6* mutant exhibited significantly higher levels of lipid peroxidation in the same growth conditions compared to controls. The *sta6* mutant was more sensitive to oxidative stress induced by H₂O₂, whereas the wild-type was relatively more resistant. In addition, significantly up-regulated autophagy-related factors including *ATG1*, *ATG101*, and *ATG8* were maintained in the *sta6* mutant regardless of nitrogen availability. Also, the *sta6* mutant exhibited relatively higher ATG8 protein level compared to wild-type under non-stress condition, and quickly reached a saturation point of autophagy when H₂O₂ was applied. Our results indicate that, in addition to the impact of carbon allocation, the increased lipid phenotype of the *sta6* mutant may result from alterations in the cellular oxidative state, which in turn activates autophagy to clean up oxidatively damaged components and fuel lipid production.

With the growing demand for environmentally friendly sustainable energy alongside an increasing world population, the subject of algal biomass production has attracted much attention since microalgae can convert atmospheric CO₂ and water pollutants into diverse value-added products including biofuel and other bioactive compounds^{1,2}. Among various compounds, algal lipid, which is mainly composed of triacylglycerol (TAG), is considered a promising resource for biodiesel production². The extracted algal lipid contents can be converted into biodiesel and glycerol via a transesterification reaction with alcohols and catalysts². Furthermore, the overexploitation of fish oil to produce bioactive fatty acids including eicosapentaenoic acid (EPA) and docosahexaenoic acid (DHA) can be solved by using microalgae as alternative resources¹. The advantages of lipid production using microalgae over terrestrial plants have already been well discussed in previous studies. Microalgae can be grown in wastewater and are able to accumulate higher lipid content with a faster growth rate than common terrestrial plants. In addition, the cultivation of microalgae does not require large areas of land, and they do not compete with general human food resources^{2,3}. However, cost-effective lipid production from microalgae remains in its infancy owing to poorly developed mass cultivation techniques and the low lipid productivity of target microalgal species. In order to promote lipid production from microalgae, many technological approaches including genetic engineering, stress regulation, and modification of cultivation apparatus have been proposed⁴⁻⁷. One of these approaches, the construction of more efficient algal mutants using genetic engineering, is considered a promising and important subject in the microalgae-to-bioproducts process⁸.

Changes made to cellular metabolic pathways via genetic modification in microalgae can enhance or reduce specific metabolite production, thereby artificially promoting lipid production. Among several strategies, enhancing algal lipid production by altering the starch biosynthesis pathway has been the most widely

¹Cell Factory Research Center, Korea Research Institute of Bioscience and Biotechnology (KRIBB), Daejeon, 34141, Republic of Korea. ²Department of Environmental Biotechnology, KRIBB school of Biotechnology, Korea University of Science & Technology (UST), Daejeon, 34113, Republic of Korea. ³Environmental Safety Group, Korea Institute of Science and Technology (KIST) Europe, Campus E 7.1, Saarbrücken, 66123, Germany. Quynh-Giao Tran and Kichul Cho contributed equally. Correspondence and requests for materials should be addressed to H.-S.K. (email: hkim@kribb.re.kr)

used technique in diverse microalgal candidates. According to de Jaeger *et al.*, genomic DNA of the freshwater microalga *Scenedesmus obliquus* was randomly modified by UV light irradiation to obtain a starchless mutant, which exhibited enhanced lipid accumulation compared to the wild-type under nitrogen-depleted conditions⁹. In addition, Li *et al.* also reported that the starchless *C. reinhardtii* mutant BAFJ5 (referred to as *sta6*), which is defective in ADP-glucose pyrophosphorylase, exhibited approximately 10-fold higher TAG accumulation than the wild-type¹⁰. Considerable efforts have been made to address the allocation of carbon toward lipids in mutants by modifying their starch biosynthesis metabolism^{9,10}. However, little attention has been paid to the regulation of autophagy and the stress response in these genetically modified algal strains.

It has been previously reported that most microalgal species can accumulate increased lipid content under stress conditions, such as nitrogen starvation, oxidative stress and high salinity¹¹. For instance, Yilancioglu *et al.* showed a halophilic microalga *Dunaliella salina* accumulated cellular lipid content and exhibited extensive lipid peroxidation under nitrogen deficiency condition, indicating high level of oxidative stress¹². The study also confirmed that hydrogen peroxide, an oxidative stress inducer, significantly induced algal lipid accumulation¹². Additionally, H₂O₂ treatment and UV irradiation has been shown to enhance lipid production in *Scenedesmus* sp.¹³. These studies suggest that lipid accumulation is highly influenced by oxidative stress in microalgae. Although the exact mechanism of this widespread phenomenon has not yet been elucidated, lipid accumulation has been linked to an increase in reactive oxygen species (ROS) along with the degradation of cellular protein components in various algal species^{11,12,14}. On the other hand, ROS-mediated stress responses and protein turnover are closely related to the autophagy mechanism^{15–17}. Autophagy is a highly conserved catabolic process that regulates cellular component degradation and recycling in a wide range of eukaryotic organisms¹⁶. Since it is considered that autophagy plays a significant role in the stress response of eukaryotic cells, the study of the relationship between ROS-mediated stress and autophagy induction is essential^{18,19}. Recently, Couso *et al.* demonstrated that maintaining normal autophagic flux is essential for lipid production in *C. reinhardtii*¹⁵. Based on previous studies, it is hypothesized that cellular stress levels and the subsequent regulation of autophagy may also be correlated with an enhanced TAG accumulation in starchless mutants. Since this has not yet been concretely investigated, in the present study, we examined the nitrogen starvation-induced oxidative stress response and autophagy regulation in the starchless *sta6* mutant of *C. reinhardtii*.

Results and Discussion

Confirmation of experimental algal strains. In order to confirm the starch phenotype of the experimental strains, wild-type (WT), complemented *STA6* mutant (*STA6-C6*) and starchless mutant (*sta6*) were spotted on plates with or without a nitrogen source, and subsequently stained with iodine vapour as described in the Materials and Methods section. As shown in Fig. 1a, we could observe a dark-brown colour in WT and *STA6-C6* colonies under N-depleted conditions, whereas *sta6* colonies exhibited an opaque yellowish green colour indicating that starch could not be produced in this mutant. Additionally, the levels of lipid droplet accumulation in WT, *STA6-C6* and *sta6* cells under N-depletion was also compared (Fig. 1b,c) to verify the ability to accumulate high amount of TAG of the *sta6* mutant as described previously^{10,20}. As shown in Fig. 1b, the number of Nile Red-stained lipid droplets in the *sta6* mutant was more pronounced compared to WT and *STA6-C6* mutant at 24 h after nitrogen starvation. In addition, fluorescence-based microplate assays revealed an approximate 5-fold and 8-fold increase in Nile Red fluorescent intensity in *sta6* cells at 24 h and 48 h post-starvation, respectively. Neutral lipid content of the control cells was also changed in response to nitrogen starvation but less significant compared to that observed in the *sta6* mutant.

Change of daily growth and stress responses. After confirmation of the *sta6* mutant, daily growth tests were performed in TAP medium. As shown in Fig. 2a, the growth curves based on algal cell concentration of WT, *STA6-C6* and *sta6* mutant were exponential up to day 3 before reaching a stationary phase that was maintained with a cell density of approximately 2×10^7 cells/ml. The total nitrogen concentration was rapidly undermined at day 3 of cultivation, then slightly reduced thereafter as the cells entered the stationary growth phase (Fig. 2b). Based on these results, we considered that limiting nitrogen in the medium might induce algal cells to enter stationary growth phase after day 3.

Previous studies have reported that microalgae cultivated under nitrogen limiting conditions increased cellular ROS levels along with enhanced lipid accumulation, and the elevated ROS may inhibit algal growth by causing cellular damage^{12,21}. Therefore, we measured the production of malondialdehyde (MDA), which is considered a marker of lipid peroxidation caused by enhanced oxidative stress, in algal samples collected at day 2 and day 4. As shown in Fig. 2c, the MDA content of WT cells was increased at day 4 compared to that at day 2 of cultivation, indicating the occurrence of lipid peroxidation and oxidative stress in stationary-phase cells. Interestingly, the *sta6* mutant showed significantly higher MDA levels than WT and *STA6-C6* cells at the same growth phase, and a high level of MDA was observed even under optimal growth conditions (day 2 sample). These results suggest that the *sta6* mutant was likely exposed to higher oxidative stress levels compared to control cells growing in the same conditions.

Thus, as a further experiment, we compared the cellular sensitivity of WT, *STA6-C6* and *sta6* to H₂O₂-induced oxidative stress conditions. Cells were grown to exponential phase and cell concentration was adjusted to 1×10^6 cells/ml before treating with H₂O₂ to induce oxidative stress (Fig. 3). The concentrations of H₂O₂ higher than 250 μ M rapidly triggered cell death in the *sta6* mutant within 16 h (Fig. 3a). Cell viability of the *sta6* mutant were $77.5 \pm 3.5\%$, $60.0 \pm 7.1\%$, $42.5 \pm 10.6\%$ and $22.5 \pm 3.5\%$ at 250, 500, 1,000 and 2,000 μ M H₂O₂, respectively. In contrast, WT and *STA6-C6* cells exhibited relatively higher resistance to H₂O₂-induced cell death (less than a 25% and 40% decrease in viability at 1,000 and 2,000 μ M H₂O₂, respectively). These results indicate that the *sta6*

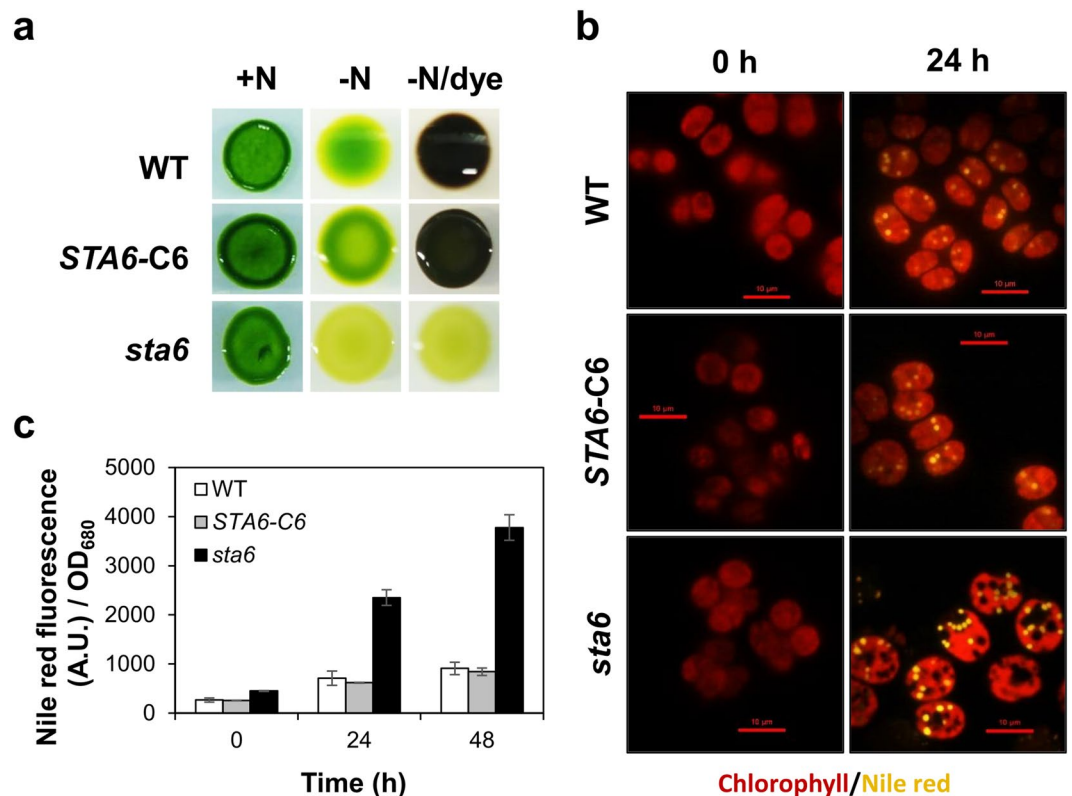


Figure 1. Confirmation of experimental algal strains. **(a)** Wild-type (WT), complemented *STA6* mutant (*STA6-C6*) and starchless mutant (*sta6*) were plated on N-depleted TAP medium for 7 days and the plates were incubated with iodine vapor. WT and *STA6-C6* colonies were stained to dark brown, indicating the presence of starch. In contrast, the *sta6* mutant was an opaque yellowish green, meaning that they failed to synthesize starch molecules. **(b)** Observation of lipid accumulation in *Chlamydomonas* cells under nitrogen starvation. Lipid droplets stained with Nile Red (yellow) and algal auto-fluorescence (red) are shown. Scale bar = 10 μ m. **(c)** Relative Nile Red fluorescence normalized to optical density (OD_{680}) of algal cells during a time course of nitrogen starvation. Error bars represent 95% confidence intervals of the means of three independent replicates. The overlapping confidence intervals indicate no significant difference.

mutant is more sensitive to oxidative stress compared to the WT and complemented *STA6* mutant, which is in accordance with the elevated cellular MDA content observed earlier.

Effects of H_2O_2 on neutral lipid accumulation in *Chlamydomonas reinhardtii*. Treatment with H_2O_2 has been shown to effectively enhance lipid yield in *D. salina* and *Scenedesmus* sp.^{12,13}. Indeed, the addition of H_2O_2 to the culture medium caused an increase in intracellular ROS levels in a wide range of organisms^{22–24}. As cellular signalling molecules, the accumulated ROS may act as potent inducers of multiple metabolic functions including lipid metabolism and autophagy²⁵. To determine whether the increased lipid accumulation in the *sta6* mutant correlates with its distinct oxidative profile, the cells in Fig. 3a were stained with DCFH-DA and fluorescence-based microplate was used to measure cellular ROS levels. The ROS contents were increased in a dose-dependent manner with H_2O_2 concentration in all strains (up to 500 μ M H_2O_2 in case of *sta6* mutant) (Fig. 3b). At the concentrations of H_2O_2 higher than 500 μ M, the *sta6* mutant had no increase in ROS levels but dramatic increase in cell death, indicating that *sta6* cells have reached an oxidative saturation point where the level of ROS exceeds cellular defence capacitance. Notably, we observed a correlation between increased neutral lipid content and increased cellular ROS levels in controls and *sta6* mutant (except for the 2,000 μ M H_2O_2 condition). As shown in Fig. 3c, with WT cells exposed to increasing amounts of H_2O_2 , lipid content increased from 271.2 ± 15.5 A.U. (non-treated control) to a maximum of 447.5 ± 23.2 A.U. (at 1,000 μ M H_2O_2) (A.U. means arbitrary units). The changes in Nile Red fluorescence intensity for the *sta6* mutant were more pronounced compared to that observed in WT and *STA6-C6* cells, which showed a positive, yet saturating relationship with the changes in its ROS levels (Fig. 3c). These results suggest that the overproduction of ROS in the *sta6* mutant may contribute to its elevated lipid accumulation.

Differential autophagic activity in the *sta6* mutant. Autophagy is a catabolic process that usually occurs in eukaryotic organisms subjected to stress. The damaged cellular organelles caused by increased ROS are degraded and recycled via autophagic activity to maintain cellular homeostasis²⁶. While the degradation of cellular materials is performed by the lysosome in animal cells, the same function is performed by lytic vacuoles in microalgae, fungi and plant cells²⁷. As discussed in a previous review²⁸, the autophagic machinery of

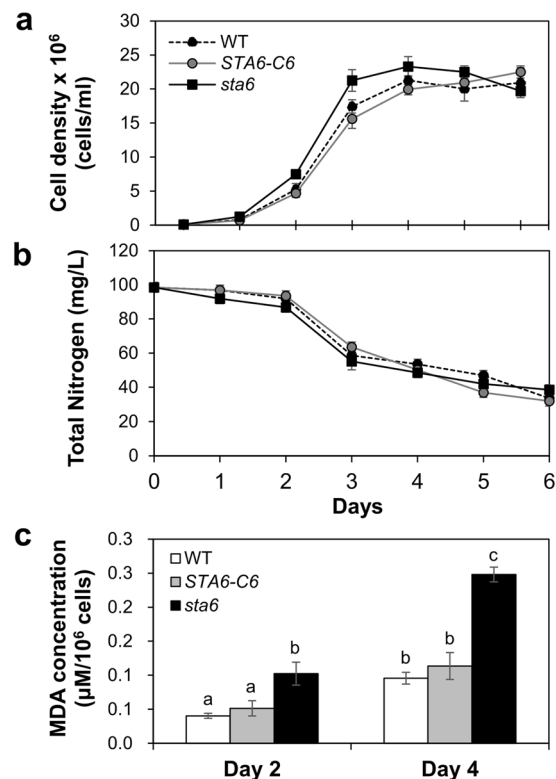


Figure 2. Comparison of growth rate and stress responses in *Chlamydomonas* strains. (a) Wild-type (WT), complemented *STA6* mutant (*STA6-C6*) and starchless mutant (*sta6*) exhibited similar growth patterns under optimal growth conditions. (b) Total nitrogen content in the medium gradually decreased correlating to algal growths. (c) The MDA contents were measured at day 2 (exponential phase) and day 4 (stationary phase) under batch culture conditions. The *sta6* mutant showed significantly higher stress levels compared to WT and *STA6-C6* cells at the same growth stage. Data represent the mean \pm standard deviation (SD). Means with the same letter are not significantly different from each other ($P > 0.05$ by *t*-test using Excel 2016 program).

Chlamydomonas comprises numerous autophagy-related (ATG) proteins. In the case of macroautophagy, hereafter referred to as autophagy, a double-membrane vesicle called the autophagosome is formed via a complicated mechanism. Autophagosome formation begins by the activation of the ATG1 complex composed of ATG1, ATG13 and probably ATG101^{28,29}. ATG101, as previously described in the model terrestrial plant *Arabidopsis thaliana*, may help link the ATG1 initiation complex to autophagic membranes³⁰. The phosphorylation of ATG1 triggers the formation of a phagophore assembly site (PAS) through phosphoinositide 3-kinase (PI3K) nucleation complex and phosphatidylinositol 3-phosphate (PI3P) binding complex. PI3K (VPS34) plays an important role in converting phosphatidylinositol (PI) to PI3P, which is required for the recruitment of other ATG proteins onto the autophagosome membrane. Among ATG proteins, ATG8 is essential for the formation of the autophagosome, while ATG7 is an E1-like enzyme involved in the activation of ATG8^{28,30,31}.

In this study, we measured the expression levels of *ATG1*, *PI3K*, *ATG101*, *ATG7* and *ATG8* genes to evaluate autophagy regulation in the *sta6* mutant (Fig. 4). Compared to the expression levels of WT (marked as dash lines), all the autophagy-related genes in the *sta6* mutant showed higher values at both day 2 and day 4. Furthermore, the *ATG1* and *ATG101* genes, which regulate the early steps of the autophagic process, were significantly up-regulated in *sta6* cells after 4 days of cultivation, whereas *ATG7* and *PI3K* has shown no statistically significant changes. Moreover, the expression levels of the *ATG8* gene were significantly promoted in samples collected at D4 (when the cells reached stationary phase). Previous studies have demonstrated that increased cellular ROS may lead to the activation of *ATG1* and subsequent autophagy by either targeting rapamycin (TOR)-dependent or TOR-independent signalling¹⁶. Thus, the enhanced expression levels of those autophagy-related genes suggested that the *sta6* mutant activated autophagy mechanism to cope with its elevated oxidative stress levels.

In addition, Western blot analysis was performed to examine the expression pattern of ATG8 protein in the *sta6* mutant. ATG8 appeared as a faint band on the blot of WT and *STA6-C6* cells grown under optimal conditions (Fig. 5a, 0 μ M H₂O₂). The abundance of ATG8 increased upon exposure to H₂O₂-induced autophagy in both controls and the *sta6* mutant (Fig. 5a). The quantification of protein band intensity was performed using ImageJ, claiming a significant increase of ATG8 protein in the *sta6* cells compared with WT or *STA6-C6* mutant subjected to the same amount of stressor (Fig. 5b). Moreover, the dose-dependent expression pattern of ATG8 protein, observed in WT and *STA6-C6* cells, was less significant in the *sta6* mutant (Fig. 5a,b). It seems that oxidative stress induces autophagy more strongly in the *sta6* mutant compared with WT and *STA6-C6* mutant.

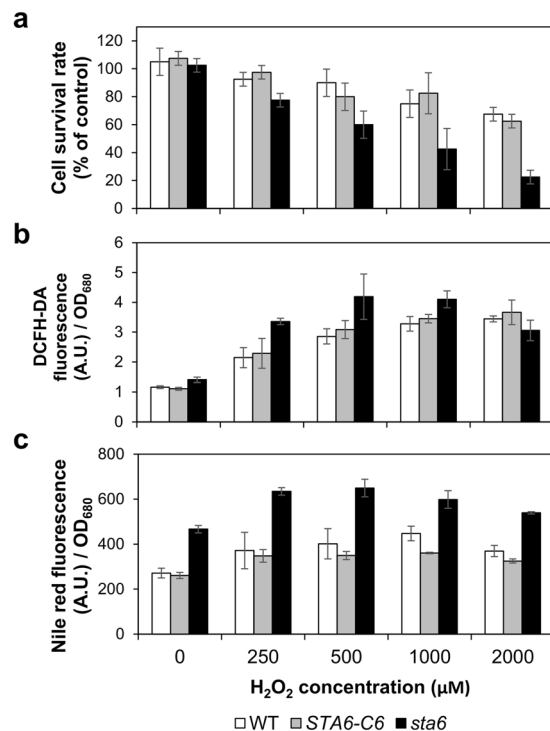


Figure 3. Effect of hydrogen peroxide (H₂O₂) on cell viability and lipid accumulation in *C. reinhardtii*. (a) Wild-type (WT), complemented *STA6* mutant (*STA6-C6*) and starchless mutant (*sta6*) were treated with H₂O₂ for 16 h and percentage of viable cells was determined. (b) Relative DCFH-DA fluorescence normalized to optical density (OD₆₈₀) of algal cells after 6 h of H₂O₂ treatment. (c) Relative Nile Red fluorescence normalized to OD₆₈₀ of algal cells after 16 h of H₂O₂ treatment. Error bars represent 95% confidence intervals of the means of three independent replicates. The overlapping confidence intervals indicate no significant difference.

Based on these results, we propose that the high lipid accumulation in the *sta6* mutant could be explained from the perspective of stress responses and autophagy regulation, alongside carbon allocation as described previously. Although the underlying mechanism remains to be clarified, we speculate that the absence of starch biosynthesis likely led to increased levels of ROS and oxidative stress in the *sta6* mutant. Subsequently, the increased cellular ROS levels could act as autophagy inducers, leading to an enhanced recycling of cellular materials and ROS-damaged components to fuel lipid production in this mutant.

It has been reported that corn, which contains high levels of amylose, one of the two components of starch, has a good antioxidant capacity³². Also, largemouth bass *Micropterus salmoides* fed with pea starch and high-amylose maize starch showed a lower MDA content and reduced oxidative stress levels³³. Similarly, oxidative stress suppression by resistant starch diet was also reported by Vaziri *et al.*³⁴. In addition, starch biosynthesis has been shown to be an essential protection mechanism against photooxidative damage in *C. reinhardtii*³⁵. The continuous generation of the reductant NADPH as an end product of the light reactions of photosynthesis leads to cellular over-reduction and the formation of ROS by transferring one electron from NADPH to oxygen³⁶. In photosynthetic cells, ATP and NADPH produced by the light reactions are used to form sugars from carbon dioxide (CO₂) via the Calvin cycle, and these sugars are further condensed into insoluble starch which has a lower osmotic pressure³⁷. By consuming excess NADPH, the production of starch allows the algae to maximize light harvesting while regenerating NADP⁺ from NADPH which can accept electrons and thus reduce the generation of ROS³⁵. Since lipid biosynthesis is the second NADPH-consuming process, an increased rate of lipid production in the *sta6* mutant would allow the cells to lower the NADPH pool^{38,39}. In fact, the levels of oxidative damage in the *sta6* mutant were still significantly higher than that in the WT cells despite its elevated lipid accumulation. Juergens *et al.* highlighted that in *C. reinhardtii* starch is primarily produced from CO₂ via photosynthesis, whereas the synthesis of fatty acids mostly relies on exogenous acetate and the turnover of membrane lipids⁴⁰. Hence, this indicated that starch plays a more important role in the protection of the photosynthetic machinery from photooxidative damage than other bioproducts, including lipids and proteins^{35,40}. Taken together, this suggests that one possible reason for the increase in lipid peroxidation in the *sta6* mutant may be the unbalanced redox state of the cells, leading to an elevated generation of ROS due to the lack of the starch biosynthesis pathway.

Conclusion

Superior lipid accumulation in starchless mutants has been generally linked to increased carbon allocation towards the lipid metabolism in previous studies. This work has expanded on those findings from a different perspective, specifically focusing on the stress response and autophagy regulation. The increased lipid peroxidation observed in *sta6* cells growing under the same conditions as WT suggests that algal cells with impaired starch

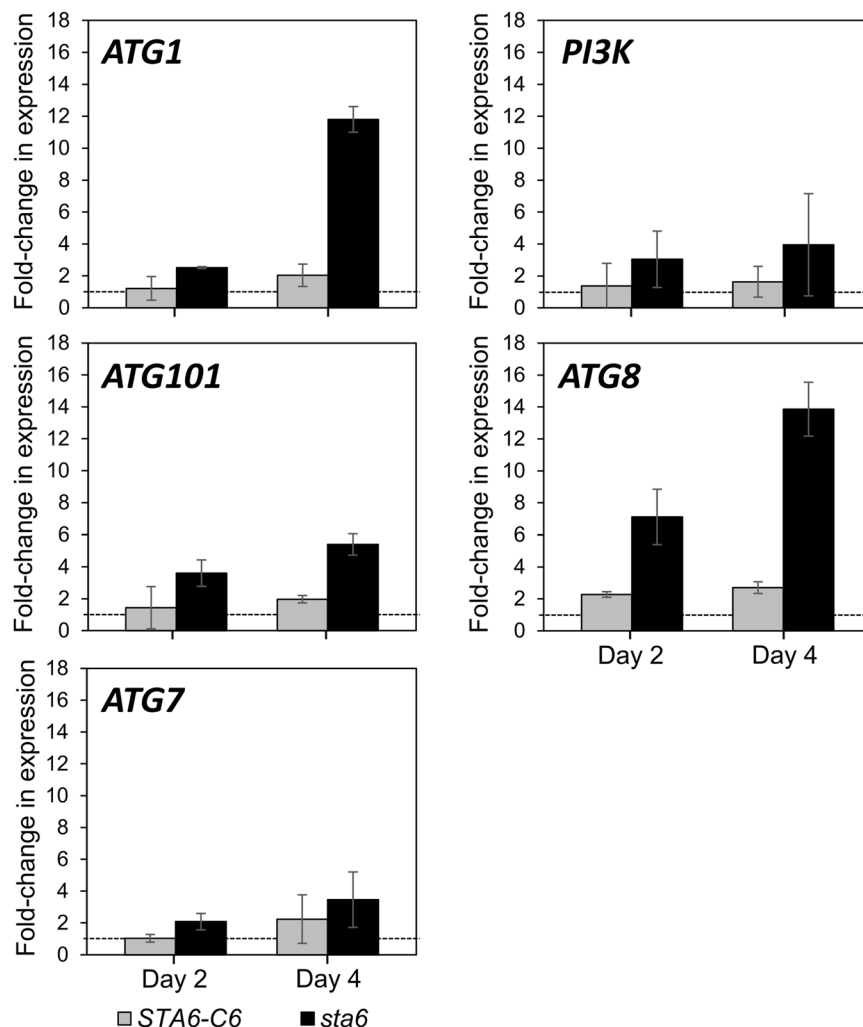


Figure 4. Expression levels of genes belonging to autophagy pathways. Transcript levels of autophagy-related (*ATG*) genes were measured by real-time qPCR in algal samples at day 2 (exponential phase) and day 4 (stationary phase). Relative expression levels of *ATG1*, *PI3K*, *ATG101*, *ATG8* and *ATG7* genes are shown. All results were normalized to *CBLP* (house-keeping gene). The bars represent the fold-change in expression of the target gene in *STA6-C6* and *sta6* relative to wild-type. The dashed line indicates the expression level of corresponding genes in wild-type. Mean values of two biological replicates were obtained using the medians of three technical replicates. Error bars represent 95% confidence intervals. The overlapping confidence intervals indicate no significant difference.

metabolism need to cope with elevated oxidative stress levels. The increased cellular ROS levels in *sta6* cells, therefore, could play a dual role as signals to trigger lipid biosynthesis and as autophagy inducers to activate the recycling of cellular components to fuel lipid production in this mutant. More research is needed to understand the antioxidant capability of purified algal starch molecules, and their roles in the regulation of related cellular pathways.

Materials and Methods

Microalgal growth conditions. *Chlamydomonas reinhardtii* CC-124 wild-type, complemented *STA6* mutant (referred to as *STA6-C6*) and starchless mutant BAF5 (referred to as *sta6*) were obtained from the *Chlamydomonas* Resource Center located at the University of Minnesota. In the *sta6* mutant, the small subunit of ADP-glucose pyrophosphorylase was deficient and the starch content was not detectable⁴¹.

Cells were grown in Tris-acetate phosphate (TAP) medium⁴² under continuous illumination of $50 \pm 10 \mu\text{mol}/\text{m}^2/\text{sec}$ at 25°C , with constant shaking at 90 rpm. For growth rate comparison, cells were initially inoculated at a density of approximately 8×10^4 cells/ml, and cell density was monitored daily using a haemocytometer.

For the nitrogen depletion studies, cells in exponential phase (at a density of approximately 1×10^6 cells/ml) were harvested by centrifugation ($2,000 \times g$ for 5 min). The cell pellet was washed twice in nitrogen-free TAP medium before resuspension in the same fresh medium at the same cell density.

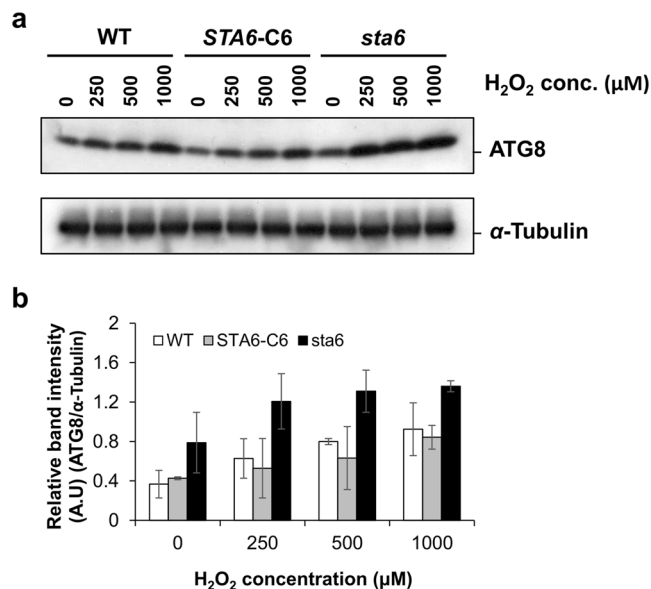


Figure 5. Differential autophagic responses in wild-type and starchless mutant. **(a)** Western blot analysis of ATG8 levels in wild-type (WT), complemented *STA6* mutant (*STA6-C6*) and starchless mutant (*sta6*) treated with H₂O₂ at concentrations of 250, 500, 1000 μM. α-tubulin is shown as a loading control. Although cropped, all blots are derived from the same gel. After transfer, the membrane was cut horizontally in half. The top half of the membrane was used to detect α-tubulin (molecular weight of approx. 50 kDa) and the bottom half was used to detect ATG8 protein (molecular weight of approx. 15 kDa). Corresponding uncropped blots with multiple exposures shown in Supplementary Figs S1 and S2. **(b)** Quantification of band intensities in **(a)** was performed using ImageJ. The band intensity of ATG8 was normalized to the according α-Tubulin and the ATG8/α-Tubulin ratios were displayed. Error bars represent 95% confidence intervals of the means of three independent replicates. The overlapping confidence intervals indicate no significant difference.

Determination of algal starch content using iodine vapor staining. Pure elemental iodine crystals (Junsei Chemical Co., Ltd., Japan) were placed on a watch glass and heated slightly to generate iodine vapor inside a fume hood. To control the staining time, WT, *STA6-C6* and *sta6* cells were spotted on the same plate. Agar plates containing algal colonies were placed on top of the watch glass for 30 s. Images were captured immediately after staining.

Analysis of total nitrogen. Algal culture broth was filtered through a 0.2 μm pore-size membrane filter (Minisart, Sartorius Stedim Biotech, Germany) before measurement. The concentration of total nitrogen (TN) was determined using Nitrogen (total) Cell Test kit (Merck, Germany) in accordance with the manufacturer's protocol.

Determination of lipid peroxidation. Lipid peroxidation products are widely used to represent the levels of oxidative stress in cells. In this study, the thiobarbituric acid reactive substance (TBARS) assay was used to quantify the level of MDA content in microalgal cells (modified from⁴³). Briefly, 1 ml samples with known number of cells were harvested by centrifugation at 2,000 × g for 5 min. Cell pellets were washed twice with cold phosphate buffered saline (PBS, pH 7.4) and resuspended in lysis buffer at a density of approximately 1 × 10⁶ cells/ml. Lysis buffer was prepared by mixing 1 μl of 10 mM butylated hydroxytoluene (BHT) solution per 100 μl of radio-immunoprecipitation assay (RIPA) buffer. The cell mixture was bead beaten at 4,500 × g for 1 min. Acid treatment was performed by adding 100 μl of 0.6 N trichloroacetic acid (TCA) solution per 100 μl of cell lysate and incubating at room temperature for 15 min. After centrifugation at 10,000 × g for 5 min, the supernatants were immediately assayed. The TBARS assay was performed by mixing 150 μl of each sample or MDA standard with 75 μl of 0.5% (w/v) thiobarbituric acid reagent. The optical density (OD) was determined at 532 nm immediately (pre-read OD₅₃₂) and after incubating for 2 h at 45–50 °C. Pre-read OD₅₃₂ was subtracted from the final read to obtain data, and MDA contents were calculated based on the MDA standard curve. The results are expressed as μM MDA/10⁶ cells.

RNA extraction, cDNA synthesis, and real-time PCR. Cell culture was harvested by centrifugation at 2,000 × g for 5 min and the pellet was immediately frozen in liquid nitrogen and stored at –80 °C. Total RNA was extracted using RNeasy Mini Kit (QIAGEN, Germany) in accordance with the manufacturer's protocol. To eliminate genomic DNA contamination, RQ1 RNase-Free DNase kit (Promega, United States) was used. RNA purity and quantity were checked with the NanoPhotometer[®] P360 device (Implen, Germany), and RNA integrity was confirmed on agarose gel by electrophoresis. Then, 500 ng of total RNA was converted to first-strand cDNA in a 20 μl reaction using GoScript[™] Reverse Transcription System (Promega, United States) with oligo (dT) primer. The generated cDNA was diluted five times with RNase-Free water, and 1 μl of this solution was used as template for real-time PCR using iQ[™] SYBR[®] Green Supermix (Biorad, United

States). The following primers were used: ATG1_F (5'-GGGTGCGGTGGTGTACTAGC-3') and ATG1_R (5'-AGTCCTCTCCGGCACCGAT-3'); PI3K_F (5'-AGGAGATGATCGAGGCCATGGG-3') and PI3K_R (5'-CCGGAACCTGTCTGCAGCTTG-3'); ATG101_F (5'-CTTCTGTGCCAGGTTGACAAGC-3') and ATG101_R (5'-GCTCAACACCCACGTTTCCAG-3'); ATG7_F (5'-GCATTGTAGGAGGTTGGTAGGAG-3') and ATG7_R (5'-CTCCAGGTCTGTGTGGCTAGCTC-3'); ATG8_F (5'-CAGCATCTCCACAATGGTTGGC-3') and ATG8_R (5'-CTCTGCCTTCTCGACAATGACTGG-3').

Western blot analysis. Cell lysates were prepared using RIPA buffer supplemented with Protease Inhibitor Cocktail (Sigma-Aldrich, United States). Then, 30 µg of total soluble protein per sample were separated on 15% SDS-PAGE gels and transferred onto a polyvinylidene difluoride membrane (Bio-Rad, United States) using a wet transfer system (Bio-Rad, United States). Western blot analysis was performed with anti-CrATG8 (Abcam, United Kingdom) and anti- α -tubulin (Sigma-Aldrich, United Kingdom) antibodies (1:2,000). The Clarity™ Western ECL Substrate (Bio-Rad, United States) was used to detect ATG8 and α -tubulin with anti-rabbit (Abcam, United Kingdom) and anti-mouse (Abcam, United Kingdom) secondary antibodies (1:10,000), respectively.

Algal lipid droplet observation by fluorescence microscope. *Chlamydomonas* cells were subjected to nitrogen starvation and microscopic observation was performed at 24 h and 48 h post-treatment. Lipid droplets were stained with Nile Red (Thermo Fisher, United States) and observed using a fluorescence microscope (Eclipse 80i, Nikon, Japan) at excitation 450–500 nm (blue laser) and emission 528 nm wavelength. Chlorophyll *a* (Chl *a*) auto-fluorescence was observed using the same filter.

Fluorescence-based microplate assays for measurement of ROS levels and lipid contents. For quantification of cellular ROS levels, algal cells were treated with different H₂O₂ concentration and stained with dichloro-dihydro-fluorescein diacetate (DCFH-DA) (Sigma-Aldrich, United Kingdom). After cells were harvested and washed twice with PBS buffer (pH 7.0), DCFH-DA was added to final concentration of 10 µM and incubated for 30 min in the dark, at 25 °C, with constant shaking at 50 rpm. The DCFH-DA signals were then measured by a fluorescence microplate reader at excitation 485 nm and emission 535 nm wavelength.

For quantification of neutral lipid content, Nile Red was added to final concentration of 1 µg/ml and incubated for 30 min in the dark at 25 °C. The Nile Red signals were measured at excitation 560 nm and emission 635 nm wavelength. All experiments were performed in triplicates. Data were normalized against OD₆₈₀ and the ratio of DCFH-DA fluorescence/OD₆₈₀ or Nile Red fluorescence/OD₆₈₀ are shown.

Statistical analysis. All data are presented as means \pm (1.96 \times standard error (SE)) for a 95% confidence interval (unless otherwise indicated). The overlapping error bars indicate no significant difference. Pairwise comparisons of data from different experimental groups were performed using a *t*-test (Excel 2016 program, Microsoft). Statistically significant differences are represented by different letters (Fig. 2).

References

- Adarme-Vega, T. C. *et al.* Microalgal biofactories: a promising approach towards sustainable omega-3 fatty acid production. *Microb. Cell Fact.* **11**, 96 (2012).
- Chisti, Y. Biodiesel from microalgae. *Biotechnol. Adv.* **25**, 294–306 (2007).
- Raheem, A., Prinsen, P., Vuppaladadiyam, A. K., Zhao, M. & Luque, R. A review on sustainable microalgae based biofuel and bioenergy production: Recent developments. *J. Clean. Prod.* **181**, 42–59 (2018).
- Radakovits, R., Jinkerson, R. E., Darzins, A. & Posewitz, M. C. Genetic engineering of algae for enhanced biofuel production. *Eukaryot. Cell* **9**, 486–501 (2010).
- Poliner, E. *et al.* A toolkit for *Nannochloropsis oceanica* CCMP 1779 enables gene stacking and genetic engineering of the eicosapentaenoic acid pathway for enhanced long-chain polyunsaturated fatty acid production. *Plant Biotechnol. J.* **16**, 298–309 (2018).
- Ji, X. *et al.* The effect of NaCl stress on photosynthetic efficiency and lipid production in freshwater microalga—*Scenedesmus obliquus* XJ002. *Sci. Total Environ.* **633**, 593–599 (2018).
- Yun, J.-H. *et al.* Hybrid operation of photobioreactor and wastewater-fed open raceway ponds enhances the dominance of target algal species and algal biomass production. *Algal Res.* **29**, 319–329 (2018).
- Ng, I. S., Tan, S. I., Kao, P. H., Chang, Y. K. & Chang, J. S. Recent developments on genetic engineering of microalgae for biofuels and bio-based chemicals. *Biotechnol. J.* **12**, 1600644 (2017).
- de Jaeger, L. *et al.* Superior triacylglycerol (TAG) accumulation in starchless mutants of *Scenedesmus obliquus*: (I) mutant generation and characterization. *Biotechnol. Biofuels* **7**, 69 (2014).
- Li, Y. *et al.* *Chlamydomonas* starchless mutant defective in ADP-glucose pyrophosphorylase hyper-accumulates triacylglycerol. *Metab. Eng.* **12**, 387–391 (2010).
- Zienkiewicz, K., Du, Z.-Y., Ma, W., Vollheyde, K. & Benning, C. Stress-induced neutral lipid biosynthesis in microalgae—molecular, cellular and physiological insights. *Biochim. Biophys. Acta, Mol. Cell. Biol. Lipids* **1861**, 1269–1281 (2016).
- Yilancioglu, K., Cokol, M., Pastirmaci, I., Erman, B. & Cetiner, S. Oxidative stress is a mediator for increased lipid accumulation in a newly isolated *Dunaliella salina* strain. *PLoS One* **9**, e91957 (2014).
- Sivaramakrishnan, R. & Incharoensakdi, A. Enhancement of lipid production in *Scenedesmus* sp. by UV mutagenesis and hydrogen peroxide treatment. *Bioresour. Technol.* **235**, 366–370 (2017).
- Stehfest, K., Toepel, J. & Wilhelm, C. The application of micro-FTIR spectroscopy to analyze nutrient stress-related changes in biomass composition of phytoplankton algae. *Plant Physiol. Biochem.* **43**, 717–726 (2005).
- Couso, I. *et al.* Autophagic flux is required for the synthesis of triacylglycerols and ribosomal protein turnover in *Chlamydomonas*. *J. Exp. Bot.* **69**, 1355–1367 (2017).
- Pérez-Pérez, M. E., Lemaire, S. D. & Crespo, J. L. ROS and autophagy in plants and algae. *Plant Physiol.* **160**, 156–164 (2012).
- Goodson, C., Roth, R., Wang, Z. T. & Goodenough, U. Structural correlates of cytoplasmic and chloroplast lipid body synthesis in *Chlamydomonas reinhardtii* and stimulation of lipid-body production with acetate-boost. *Eukaryot. Cell*, EC. 05242–05211 (2011).
- Bellot, G. L., Liu, D. & Pervaiz, S. ROS, autophagy, mitochondria and cancer: the hidden master? *Mitochondrion* **13**, 155–162 (2013).
- Scherz-Shouval, R. & Elazar, Z. Regulation of autophagy by ROS: physiology and pathology. *Trends Biochem. Sci.* **36**, 30–38 (2011).
- Wang, Z. T., Ullrich, N., Joo, S., Waffenschmidt, S. & Goodenough, U. Algal lipid bodies: stress induction, purification, and biochemical characterization in wild-type and starchless *Chlamydomonas reinhardtii*. *Eukaryot. Cell* **8**, 1856–1868 (2009).

21. Zhang, Y.-M., Chen, H., He, C.-L. & Wang, Q. Nitrogen starvation induced oxidative stress in an oil-producing green alga *Chlorella sorokiniana* C3. *PLoS One* **8**, e69225 (2013).
22. Zmijewski, J. W. *et al.* Exposure to hydrogen peroxide induces oxidation and activation of AMP-activated protein kinase. *The Journal of biological chemistry* **285**, 33154–33164 (2010).
23. Pérez-Pérez, M. E., Lemaire, S. D. & Crespo, J. L. Reactive Oxygen Species and Autophagy in Plants and Algae. *Plant Physiol.* **160**, 156–164 (2012).
24. Perrone, G. G., Tan, S.-X. & Dawes, I. W. Reactive oxygen species and yeast apoptosis. *Biochim. Biophys. Acta, Mol. Cell. Biol. Lipids* **1783**, 1354–1368 (2008).
25. Shi, K. *et al.* Reactive Oxygen Species-Mediated Cellular Stress Response and Lipid Accumulation in Oleaginous Microorganisms: The State of the Art and Future Perspectives. *Frontiers in microbiology* **8**, 793–793 (2017).
26. Kroemer, G., Mariño, G. & Levine, B. Autophagy and the integrated stress response. *Mol. Cell* **40**, 280–293 (2010).
27. Becker, B. Function and evolution of the vacuolar compartment in green algae and land plants (*Viridiplantae*). *Int. Rev. Cytol.* **264**, 1–24 (2007).
28. Pérez-Pérez, M. E., Couso, I., Heredia-Martínez, L. G. & Crespo, J. L. Monitoring autophagy in the model green microalga *Chlamydomonas reinhardtii*. *Cells* **6**, 36 (2017).
29. Jiang, Q., Zhao, L., Dai, J. & Wu, Q. Analysis of autophagy genes in microalgae: *Chlorella* as a potential model to study mechanism of autophagy. *PLoS One* **7**, e41826 (2012).
30. Li, F., Chung, T. & Vierstra, R. D. AUTOPHAGY-RELATED11 plays a critical role in general autophagy- and senescence-induced mitophagy in *Arabidopsis*. *Plant Cell, tpc.* **113**, 120014 (2014).
31. Nascimbene, A. C., Codogno, P. & Morel, E. Phosphatidylinositol-3-phosphate in the regulation of autophagy membrane dynamics. *FEBS J.* **284**, 1267–1278 (2017).
32. Li, W., Wei, C., White, P. J. & Beta, T. High-amylose corn exhibits better antioxidant activity than typical and waxy genotypes. *J. Agric. Food Chem.* **55**, 291–298 (2007).
33. Song, M.-Q. *et al.* Effect of starch sources on growth, hepatic glucose metabolism and antioxidant capacity in juvenile largemouth bass, *Micropterus salmoides*. *Aquaculture* **490**, 355–361 (2018).
34. Vaziri, N. D. *et al.* High amylose resistant starch diet ameliorates oxidative stress, inflammation, and progression of chronic kidney disease. *PLoS One* **9**, e114881 (2014).
35. Krishnan, A. *et al.* Metabolic and photosynthetic consequences of blocking starch biosynthesis in the green alga *Chlamydomonas reinhardtii* *sta6* mutant. *Plant J.* **81**, 947–960 (2015).
36. Tripathy, B. C. & Oelmüller, R. Reactive oxygen species generation and signaling in plants. *Plant Signal. Behav.* **7**, 1621–1633 (2012).
37. Bessey, C. E. The Role of Diffusion and Osmotic Pressure in Plants. *Science* **18**, 208–209 (1903).
38. da Veiga Moreira, J. *et al.* Cell cycle progression is regulated by intertwined redox oscillators. *Theor. Biol. Med. Model.* **12**, 10 (2015).
39. Gargouri, M., Bates, P. D., Park, J.-J., Kirchoff, H. & Gang, D. R. Functional photosystem I maintains proper energy balance during nitrogen depletion in *Chlamydomonas reinhardtii*, promoting triacylglycerol accumulation. *Biotechnol. Biofuels* **10**, 89 (2017).
40. Juergens, M. T., Disbrow, B. & Shachar-Hill, Y. The Relationship of Triacylglycerol and Starch Accumulation to Carbon and Energy Flows During Nutrient Deprivation in *Chlamydomonas*. *Plant Physiol.* **171**, 2445–2457 (2016).
41. Zabawinski, C. *et al.* Starchless Mutants of *Chlamydomonas reinhardtii* Lack the Small Subunit of a Heterotetrameric ADP-Glucose Pyrophosphorylase. *J. Bacteriol.* **183**, 1069–1077 (2001).
42. Harris, E. H. In *The Chlamydomonas Sourcebook (Second Edition)*. (eds Elizabeth, H. Harris, David, B. Stern & George, B. Witman) 241–302 (Academic Press, 2009).
43. Jambunathan, N. In *Plant Stress Tolerance: Methods and Protocols*. (ed. Ramanjulu Sunkar) 291–297 (Humana Press, 2010).

Acknowledgements

This work was supported by a grant from Marine Biotechnology Program (20150184) funded by Ministry of Oceans and Fisheries, Korea; by the Advanced Biomass R&D Center (ABC) of Global Frontier Project funded by the Ministry of Science and ICT(ABC-2015M3A6A2065697); and by grant from the Korea Research Institute of Bioscience and Biotechnology (KRIBB) Research Initiative Program (www.kribb.re.kr)

Author Contributions

Q.-G.T., K.C. and H.-S.K. conceived the research plan; Q.-G.T. performed most of the experiments and analysed the data; H.-S.K. supervised the project; K.C., S.-B.P., U.K. and Y.J.L. contributed to the interpretation of the results and manuscript revision. Q.-G.T. and K.C. wrote the article with contributions of all the authors.

Additional Information

Supplementary information accompanies this paper at <https://doi.org/10.1038/s41598-019-46313-6>.

Competing Interests: The authors declare no competing interests.

Publisher's note: Springer Nature remains neutral with regard to jurisdictional claims in published maps and institutional affiliations.



Open Access This article is licensed under a Creative Commons Attribution 4.0 International License, which permits use, sharing, adaptation, distribution and reproduction in any medium or format, as long as you give appropriate credit to the original author(s) and the source, provide a link to the Creative Commons license, and indicate if changes were made. The images or other third party material in this article are included in the article's Creative Commons license, unless indicated otherwise in a credit line to the material. If material is not included in the article's Creative Commons license and your intended use is not permitted by statutory regulation or exceeds the permitted use, you will need to obtain permission directly from the copyright holder. To view a copy of this license, visit <http://creativecommons.org/licenses/by/4.0/>.

© The Author(s) 2019